Simultaneous Observation of Doubly and Triply Chloride Bridged Isomers of an Electron-Rich Ruthenium Dimer: Role of Dimer Geometry in Determining Reactivity

Samantha D. Drouin, Sebastien Monfette, Dino Amoroso, Glenn P. A. Yap, and Deryn E. Fogg*

Center for Catalysis Research and Innovation, Department of Chemistry, University of Ottawa, Ottawa, Ontario, Canada K1N 6N5

Received March 15, 2005

High-yield routes to the dimeric monocarbonyl complexes $[RuCl_2(PP)(CO)]_2$ (**3**; PP = dcypb, 1,4-bis(dicyclohexylphosphino)butane) are established via (a) decarbonylation of mononuclear $RuCl_2(PP)(CO)_2$ (**4**), (b) one-pot carbonylation−decarbonylation of $RuCl(PP)(\mu\text{-}Cl)_3Ru(PP)(N_2)$ (**1**), and, most conveniently, (c) phosphine exchange of $RuCl_2(PPh_3)_3$ with dcypb, followed by a carbonylation−decarbonylation sequence as in (b), all three steps being carried out in a one-pot procedure. One or three isomers of **3** can be observed by NMR analysis, depending on the solvent medium. A mixture of $[RuCl(PP)(CO)]_2(\mu\text{-}Cl)_2$ (transoid, **3a**; cisoid, **3b**) and ionic $\{[Ru(PP)(CO)]_2(\mu\text{-}Cl)_3\}Cl$ (**3c**) is present in benzene, chlorobenzene, or THF. In CH_2Cl_2 or $CDCl_3$, only **3c** is observed. This represents the first $Ru_2X_4L_4$ system (L = L, L′) in which three of the possible edge-bridging and face-bridging isomers can be simultaneously observed and in which their ratio can be manipulated. Reactivity studies indicate that the face-sharing isomer **3c** is considerably more stable than its edge-sharing isomers. Transformations of **3** are significantly accelerated by introduction of a donor solvent (methanol, THF). Product identities were established by ^1H, ^{13}C, and ^{31}P NMR and IR spectroscopy, by microanalysis, and by X-ray crystallography (**3a/3b**, **3c**, **4a/4b**).

Introduction

Monocarbonyl complexes of ruthenium(II) support a wide range of catalytic processes. A survey of recent studies involving the well-known hydrido carbonyl catalyst $RuHCl(PCy_3)_2(CO)$, for example, reveals high activity in olefin hydrogenation and isomerization,[1−5] hydrovinylation,[6−10] dehydrosilylation,[11] silylative coupling,[12−17] and intermolecular coupling of alkenes and amines.[18] Our interest in strongly electron-donating ligands such as alkylphosphines stems from their capacity to enhance olefin binding and activation.[19] Despite the potential for simultaneously enhancing catalyst reactivity and complex stability, Ru carbonyl complexes of *chelating,* electron-rich alkylphosphines have been underinvestigated, relative to their arylphosphine analogues. We recently described[20] the impressive activity of monoruthenium complexes containing a single CO group and an electron-rich dcypb ligand in the hydrogenation of benzophenone, a challenging[21,22a] diaryl ketone substrate. We now report that decarbonylation of $RuCl_2(dcypb)(CO)_2$ (**4**) enables development of convenient routes to dimeric **3**, effective precursors[20] to these hydrogenation catalysts.

Of fundamental interest is the observation of three distinct structural isomers of **3**: edge-sharing transoid

* To whom correspondence should be addressed. E-mail: dfogg@science.uottawa.ca. Fax: (613) 562-5170.

(1) Dinger, M. B.; Mol, J. C. *Eur. J. Inorg. Chem.* **2003**, 2827−2833.
(2) Fernando De Souza, R.; Rech, V.; Dupont, J. *Adv. Synth. Catal.* **2002**, *344*, 153−155.
(3) Lee, H. M.; Smith, D. C., Jr.; He, Z.; Stevens, E. D.; Yi, C. S.; Nolan, S. P. *Organometallics* **2001**, *20*, 794−797.
(4) Yi, C. S.; Lee, D. W. *Organometallics* **1999**, *18*, 5152−5156.
(5) Martin, P.; McManus, N. T.; Rempel, G. L. *J. Mol. Catal. A* **1997**, *126*, 115−131.
(6) He, Z.; Yi, C. S.; Donaldson, W. A. *Synlett* **2004**, 1312−1314.
(7) RajanBabu, T. V.; Nomura, N.; Jin, J.; Nandi, M.; Park, H.; Sun, X. *J. Org. Chem.* **2003**, *68*, 8431−8446.
(8) He, Z.; Yi, C. S.; Donaldson, W. A. *Org. Lett.* **2003**, *5*, 1567−1569.
(9) Yi, C. S.; He, Z.; Lee, D. W. *Organometallics* **2001**, *20*, 802−804.
(10) Yi, C. S.; Lee, D. W.; Chen, Y. *Organometallics* **1999**, *18*, 2043−2045.
(11) Yi, C. S.; He, Z.; Lee, D. W.; Rheingold, A. L.; Lam, K.-C. *Organometallics* **2000**, *19*, 2036−2039.
(12) Marciniec, B.; Chadyniak, D.; Krompiec, S. *Tetrahedron Lett.* **2004**, *45*, 4065−4068.
(13) Jankowska, M.; Marciniec, B.; Pietraszuk, C.; Cytarska, J.; Zaidlewicz, M. *Tetrahedron Lett.* **2004**, *45*, 6615−6618.
(14) Itami, Y.; Marciniec, B.; Kubicki, M. *Chem. Eur. J.* **2004**, *10*, 1239−1248.
(15) Marciniec, B.; Majchrzak, M. *J. Organomet. Chem.* **2003**, *686*, 228−234.
(16) Itami, Y.; Marciniec, B.; Majchrzak, M.; Kubicki, M. *Organometallics* **2003**, *22*, 1835−1842.
(17) Itami, Y.; Marciniec, B.; Kubicki, M. *Organometallics* **2003**, *22*, 3717−3722.
(18) Yi, C. S.; Yun, S. Y.; Guzei, I. A. *Organometallics* **2004**, *23*, 5392−5395.
(19) Valentine, D. H.; Hillhouse, J. H. *Synthesis* **2003**, 2437−2460.
(20) Drouin, S. D.; Amoroso, D.; Yap, G. P. A.; Fogg, D. E. *Organometallics* **2002**, *21*, 1042−1049.
(21) (a) Dijkstra, H. P.; Albrecht, M.; Medici, S.; van Klink, G. P. M.; van Koten, G. *Adv. Synth. Catal.* **2002**, *344*, 1135. (b) Albrecht, M.; Crabtree, R. H.; Mata, J.; Peris, E. *Chem. Commun.* **2002**, 32−33.
(22) (a) Noyori, R. *Angew. Chem., Int. Ed.* **2002**, *41*, 2008−2022. (b) Noyori, R.; Takaya, H. *Acc. Chem.* Res. **1990**, *23*, 345−50. (c) DiMichele, L.; King, S. A.; Douglas, A. W. *Tetrahedron: Asymmetry* **2003**, *14*, 3427−3429.

10.1021/om050195p CCC: $30.25
Publication on Web 09/01/2005

Scheme 1

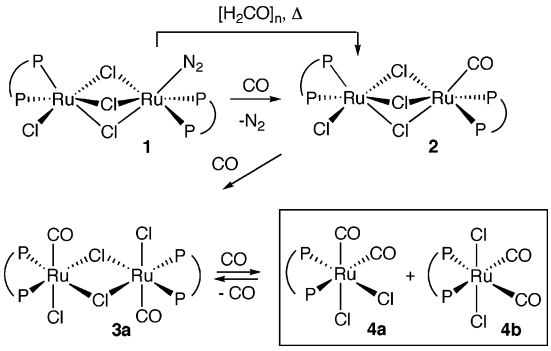

and cisoid [RuCl(dcypb)(CO)]$_2$(μ-Cl)$_2$ (**3a** and **3b**, respectively), and face-sharing ionic {[Ru(dcypb)(CO)]$_2$(μ-Cl)$_3$}Cl (**3c**). These complexes represent *incipient* sources of coordinatively unsaturated $RuCl_2L_2(CO)$, the accessibility of which depends on the lability of the dative chloride bonds that enable bridging. The catalytic activity of such coordinatively saturated dimers is thus (presuming inner-sphere catalysis) a function of the ease and rapidity with which they can release the mononuclear species. Some of the best examples of chloride-bridged dimers that exhibit potent catalytic activity are the Noyori hydrogenation catalyst, formulated as $Ru_2Cl_4(binap)_2(NEt_3)$ or NH_2Et_2\{[RuCl(binap)]$_2$(μ-Cl)$_3$\},[22] and Wilkinson's dimer, [Rh(PPh$_3$)$_2$]$_2$(μ-Cl)$_2$. In olefin metathesis, triply chloride bridged dimers function as catalytic sinks,[23] although related, doubly bridged species can exhibit high activity.[24] The accessibility of three geometrically distinct dimeric species in the present work permits direct examination of the influence of dimer geometry on reactivity. The profound influence of solvent on both stability and preferred geometry, in turn, has potentially important implications for reactivity and catalysis.

Results and Discussion

Routes to [RuCl$_2$(dcypb)(CO)]$_2$ (3). Mononuclear $RuCl_2(dcypb)(CO)_2$ (**4**) is accessible in near-quantitative yields by carbonylation of dinuclear RuCl(dcypb)(μ-Cl)$_3$Ru(dcypb)(N$_2$) (**1**) under 1 atm of carbon monoxide.[25] The reaction is presumed to proceed via RuCl(dcypb)(μ-Cl)$_3$Ru(dcypb)(CO) (**2**) and [RuCl$_2$(dcypb)(CO)]$_2$ (**3**; one isomer is shown in Scheme 1). In an attempt to arrest substitution at the stage of **3**, we used a high-vacuum line equipped with a digital Baratron capacitance manometer to introduce CO in stoichiometric amounts. These efforts were thwarted by the poor solubility of **1**, which results in a mixture that includes unreacted **1**, **2**, and overcarbonylation products **4**. The identity of **2** was confirmed by its independent synthesis via reaction of **1** with gaseous formaldehyde: this complex gives rise to two pairs of ^{31}P NMR doublets, in a pattern characteristic[26] of RuCl(PP)(μ-Cl)$_3$Ru(PP)(L) systems and indeed very similar to that found for the dinitrogen analogue **1** (for ^{31}P NMR data, see Table 1). The IR spectrum of **2** exhibits a single band for terminally bound CO at 1940 cm^{-1}, a location ca. 40 cm^{-1} lower in energy than that reported for the corresponding dppb complex (dppb = 1,4-bis(diphenylphosphino)butane),[26] consistent with the greater electron density on the metal in **2**. The identity of **2** is further supported by microanalysis, though measurement of the ^{13}C NMR spectrum was impeded by low solubility.

Table 1. ^{31}P{^{1}H} NMR Data for dcypb Complexes[a]

complex	chem shift (ppm) and coupling constant (Hz)
RuCl(dcypb)(μ-Cl)$_3$Ru(dcypb)(N$_2$) (**1**)[25]	60.1, 45.3 (AX, $^2J_{PP}$ = 40); 49.1, 37.4 (AX, $^2J_{PP}$ = 26)
RuCl(dcypb)(μ-Cl)$_3$Ru(dcypb)(CO) (**2**)	59.6, 43.7 (AX, $^2J_{PP}$ = 40); 50.4, 43.0 (AX, $^2J_{PP}$ = 23)
transoid-[RuCl(dcypb)(CO)]$_2$(μ-Cl)$_2$ (**3a**)	40.6 (s) or 34.4 (s)
cisoid-[RuCl(dcypb)(CO)]$_2$(μ-Cl)$_2$ (**3b**)	40.6 (s) or 34.4 (s)
[Ru(dcypb)(CO)]$_2$(μ-Cl)$_3$]Cl (**3c**)[b]	55.3, 42.3 (AX, $^2J_{PP}$ = 23)
ccc-RuCl$_2$(dcypb)(CO)$_2$ (**4a**)	39.4, 17.1 (AX, $^2J_{PP}$ = 22)
tcc-RuCl$_2$(dcypb)(CO)$_2$ (**4b**)	13.8 (s)

[a] Values in C_6D_6 at 121 MHz. [b] In $CDCl_3$: δ_P 50.8, 42.5 (AX, $^2J_{PP}$ = 23 Hz); δ_C 200.3 (t, $^2J_{PC}$ = 15 Hz).

Puerta, Caulton, and co-workers have discussed the difficulty of restraining carbonylation in the synthesis of highly reactive $RuX_2L_2(CO)$ complexes.[27] Synthesis of **3** presents a parallel problem, differing only in the fact that the cis disposition of the chloride ligands (imposed by cis chelation of the diphosphine ligand) facilitates dimerization. In either case, a limitation on the source of CO is essential: hence, in earlier work, we resorted to synthesis of **3** via phosphine exchange of $RuCl_2(PPh_3)_2(CO)(DMF)$ with dcypb.[20] We were prompted to examine *decarbonylation* of **4** as a potentially more convenient route to **3** by the serendipitous crystallization of the latter (as edge-sharing isomers **3a**/**3b**; vide infra) from benzene solutions of **4** that had been left to stand for several weeks under N_2. X-ray-quality crystals of mononuclear **4a**/**4b** were obtained from the same solution over a shorter period: at no point were signals for **3** observable by ^{31}P NMR analysis of the mother solution. Precedent exists for photochemical scission of Ru^{II}–CO bonds on irradiation with ultraviolet[28–30] or, more rarely, visible[28] light. Formation of **3** is consistent with the pathway shown in Scheme 2, in which an equilibrium involving loss and recapture of a CO ligand is disrupted by partial loss of CO from solution. Such a mechanism underlies the well-established isomerization of $RuCl_2L_2(CO)_2$ complexes,[28,31,32] as well as the dimerization chemistry.

(23) (a) Amoroso, D.; Yap, G. P. A.; Fogg, D. E. *Organometallics* **2002**, *21*, 3335–3343. (b) Amoroso, D.; Snelgrove, J. L.; Conrad, J. C.; Drouin, S. D.; Yap, G. P. A.; Fogg, D. E. *Adv. Synth. Catal.* **2002**, *344*, 757–763.

(24) (a) Volland, M. A. O.; Hansen, S. M.; Rominger, F.; Hofmann, P. *Organometallics* **2004**, *23*, 800–816. (b) Hansen, S. M.; Volland, M. A. O.; Rominger, F.; Eisentrager, F.; Hofmann, P. *Angew. Chem., Int. Ed.* **1999**, *38*, 1273–1276.

(25) Amoroso, D.; Yap, G. P. A.; Fogg, D. E. *Can. J. Chem.* **2001**, *79*, 958–963.

(26) Joshi, A. M.; Thorburn, I. S.; Rettig, S. J.; James, B. R. *Inorg. Chim. Acta* **1992**, *198–200*, 283–296.

(27) Marchenko, A. V.; Huffman, J. C.; Valerga, P.; Jimenez Tenorio, M.; Puerta, M. C.; Caulton, K. G. *Inorg. Chem.* **2001**, *40*, 6444–6450.

(28) Barnard, C. F. J.; Daniels, J. A.; Jeffery, J.; Mawby, R. J. *J. Chem. Soc., Dalton Trans.* **1976**, 953–961.

(29) Barnard, C. F. J.; Daniels, J. A.; Jeffery, J.; Mawby, R. J. *J. Chem. Soc., Dalton Trans.* **1976**, 1861–1864.

(30) Deacon, G. B.; Kepert, C. M.; Sahely, N.; Skelton, B. W.; Spiccia, L.; Thomas, N. C.; White, A. H. *J. Chem. Soc., Dalton Trans.* **1999**, 275–277.

(31) Krassowski, D. W.; Nelson, J. H.; Brower, K. R.; Hauenstein, D.; Jacobson, R. A. *Inorg. Chem.* **1988**, *27*, 4294–307.

(32) The tcc isomer **4b** is stable in $CHCl_3$ at 22 °C but slowly isomerizes to *ccc*-**4a** in benzene or, more rapidly, in THF (90% **4a** after 24 h in THF, +10% of an unknown byproduct at δ_P 20 ppm; 10% **4a** after 18 h in C_6D_6). Isomer **4a** does not isomerize within 24 h in these solvents.

Scheme 2

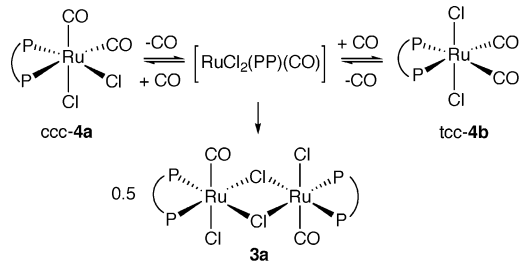

Thermolytic cleavage of metal−carbonyl bonds is more common, though isolated yields of the target dimers are quite variable (6−94%) for $RuCl_2L_2(CO)_2$ precursors (L_2 = 2 PMe*i*Pr$_2$,[27] 2 PMe_2Ph,[28] 2 $PMePh_2$,[31] dtbpe,[33] dppe;[34] dtbpe = 1,2-bis(di-*tert*-butylphosphino)-ethane, dppe = 1,2-bis(diphenylphosphino)ethane). In the extreme (as in ctc $RuCl_2(PMe_2Ph)_2(CO)_2$), the M−CO bonds are not thermally labile,[28] owing to the low trans effect of chloride. In both **4a** and **4b**, reactivity is amplified by the positioning of at least one CO ligand trans to a labilizing phosphine functionality. Accordingly, **4** is readily converted into dimeric **3** in refluxing methanol and isolated in ca. 80% yield (as the ionic isomer **3c**; vide infra) by crystallization from benzene. Of interest, particularly given the high yield of **3**, is the observation of ^{31}P NMR singlets at 23.7 and 24.0 ppm (1:1 CH_2Cl_2:MeOH; 25% of total integration) prior to crystallization. An inert-atmosphere MALDI mass spectrum of the crude reaction mixture is indistinguishable from a composite spectrum of **3** + isolated **4**: each shows an isotope pattern corresponding to the cation of **3c** and signals for [**4** − Cl − CO] and [**4** − $(CO)_2$]. We have been unable so far to isolate these intermediates, but their apparent lability, inferred from the high yields of clean **3**, and the MALDI evidence indicating a common core with **4**, point toward a species such as $RuCl_2(PP)(CO)$-(MeOH) (**5**) or possibly (by analogy to recent dtbpe chemistry)[35] {[Ru(dcypb)(CO)]$_2$(μ-Cl)$_3$}[$RuCl_3$(PP)(CO)]. Formation of a solvento species of type **5** was proposed in earlier work[34] on the basis of IR evidence; however, addition of MeOH to CD_2Cl_2 solutions of **3c** causes no change to the ^{31}P NMR spectrum, suggesting that **5** may be too labile for direct observation. We regard an alternative assignment as coordinatively unsaturated $RuCl_2$(dcypb)(CO) as improbable, in view of the ease with which the latter species may be expected to dimerize in solution. Pulsed gradient spin−echo (PGSE) diffusion studies show that "$RuCl_2$(dtbpe)(CO)" (prepared by vacuum thermolysis of $RuCl_2$(dtbpe)$(CO)_2$) exists as a dimer in solution, despite X-ray evidence for the monomeric structure in the solid state.[35]

The success of the methanolic thermolysis route[36] enabled us to prepare **3** from N_2-bound dimer **1** via a one-pot carbonylation−decarbonylation sequence. By stirring **1** under CO in methanol at room temperature and then heating the reaction to reflux under N_2, we were able to isolate clean **3** in >80% yield from **1**. The one-pot procedure can be extended to include preparation of **1** via an initial step involving phosphine exchange of dcypb with the precursor $RuCl_2(PPh_3)_3$ (Scheme 3; 72% overall yield). This last modification is particularly convenient, in that it enables synthesis of **3** from a commonly used and commercially available precursor, through a three-step reaction sequence, without isolation of intermediates **1** or **4**.

Scheme 3

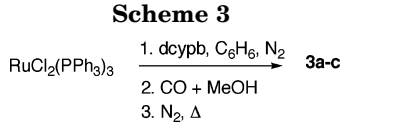

Relationship between Edge-Sharing and Face-Sharing Bioctahedra. An unexpected feature of this chemistry is the accessibility of three isomeric forms of **3** (**a**−**c**; Chart 1), the ratio of which is strongly solvent dependent.[37] We were particularly interested in the energetic relationship between the edge- and face-sharing forms of **3**, given the prevalence of the chloride-bridged structural motif in ruthenium chemistry,[38] and the solvent dependence common in catalysis via such species.[39,40]

Chart 1

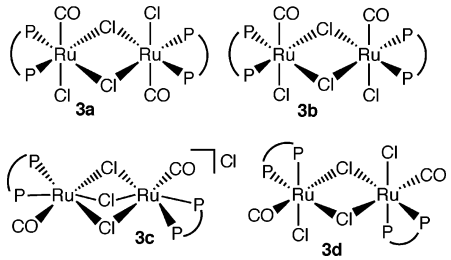

Complex **3** exists as a single isomer in chloroform or methylene chloride, as we originally reported: key characterization data include an AX pattern in the ^{31}P NMR spectrum and a triplet for the CO ligands in the ^{13}C NMR spectrum. NMR, IR, and mass spectrometric data do not distinguish, however, between the edge-sharing dimer originally proposed (**3d**, Chart 1)[20] and the ionic, face-sharing isomer **3c**. We can now unambiguously identify the species present in CH_2Cl_2 as **3c**, on the basis of experiments involving exchange of the

(33) Gottschalk-Gaudig, T.; Folting, K.; Caulton, K. G. *Inorg. Chem.* **1999**, *38*, 5241−5245.

(34) Grocott, S. C.; Wild, S. B. *Inorg. Chem.* **1982**, *21*, 3535−3540.

(35) Goicoechea, J. M.; Mahon, M. F.; Whittlesey, M. K.; Kumar, P. G. A.; Pregosin, P. S. *Dalton Trans.* **2005**, 588−597.

(36) Although control experiments carried out under an N_2 atmosphere confirm that carbon monoxide, rather than methanol, is the source of the CO ligand in **3**, use of methanol is critical for clean reaction. Thermolysis in ethanol, THF, benzene, or toluene results in contamination by varying amounts of an unknown byproduct, characterized by a ^{31}P NMR singlet at 20 ppm. (Observation of this byproduct in aromatic solvents precludes assignment as a solvento species such as **5**; vide infra.)

(37) It will be noted that none of the isomers shown for **3** in Chart 1 include a structure in which a CO ligand is trans to phosphine. Such a configuration is disfavored by the high trans effects of both of these ligand types (its appearance in **4a** and **4b** reflects the even greater thermodynamic undesirability of an alternative containing mutually trans carbonyl groups). We exclude this structural possibility for **3** on the basis of ^{31}P NMR chemical shift data (as well as signal multiplicities). As Table 1 indicates, those complexes containing mutually trans carbonyl and phosphine ligands are characterized by an unusually high-field ^{31}P NMR chemical shift, which affords a useful spectroscopic handle for structural elucidation and assignment.

(38) Seddon, E. A.; Seddon, K. R. *The Chemistry of Ruthenium*; Elsevier: Amsterdam, 1984.

(39) Bianchini, C.; Barbaro, P.; Scapacci, G.; Zanobini, F. *Organometallics* **2000**, *19*, 2450−2461.

(40) See, for example: (a) Nkosi, B. S.; Coville, H. J.; Albers, M. O.; Gordon, C.; Viney, M.; Singleton, E. *J. Organomet. Chem.* **1990**, *386*, 111−119. (b) Fogg, D. E.; James, B. R.; Kilner, M. *Inorg. Chim. Acta* **1994**, *222*, 85−90. (c) Zanetti, N. C.; Spindler, F.; Spencer, J.; Togni, A.; Rihs, G. *Organometallics* **1996**, *15*, 860−866.

chloride counterion with $TlPF_6$. This reaction effects quantitative conversion to **3c**·PF_6 (isolated in 81% yield) with no change in the AX pattern for **3c**. The face-sharing structure is confirmed by X-ray analysis.

While **3c** is the only species observed in $CHCl_3$ or CH_2Cl_2, two other isomers are also evident in benzene, chlorobenzene, or THF. These are identified as the neutral, edge-sharing dimers transoid **3a** and cisoid **3b**, also characterized by X-ray analysis following serendipitous crystallization from solutions of **4**, as noted above. ^{31}P NMR spectra of **3** in C_6D_6 thus reveal two 1:1 singlets (40.6, 34.4 ppm; Table 1) due to the edge-sharing dimers, as well as the AX spin system due to **3c**, integration of which is affected by precipitation. In chlorobenzene (in which all three isomers are soluble), their ratio is 1:1:10. We note that the related $[RuClL_2(CO)]_2(\mu\text{-}Cl)_2$ dimers (L_2 = dtbpe or 2 PMe^{i}Pr$_2$)[27,33] are also observed in two isomeric forms. The dtbpe chemistry affords a mixture of cisoid and transoid isomers, as deduced by the observation of two ^{31}P NMR singlets.[33,41] For the PMe^{i}Pr$_2$ species, an AB pattern is accompanied (though apparently not invariably)[42] by a singlet presumably due to a cisoid or transoid isomer;[27,42] the AB pattern was assigned to an isomer isostructural with **3d**,[27] though a cationic complex of the type **3c** could also account for this set of signals. In some instances, observation of a single infrared ν(CO) stretching band is adduced as evidence for a C_{2h}, rather than a C_{2v}, structure (thus **3a**, rather than **3b**).[31,34] However, mixtures of such isomers in some cases give rise to a single ν(CO) band,[27,33] as indeed is observed for **3**.

^{31}P EXSY analysis of **3** in C_6D_6 revealed a correlation between the signals for **3a** and **3b**, indicating that the edge-sharing isomers are related by a chemical equilibrium.[43] No correlation of these signals with those due to **3c** is evident, indicating that the edge−face interconversion is slow on the NMR time scale. Chemical evidence, however, confirms that all three isomers exist in equilibrium (Scheme 4). This evidence includes (a)

Scheme 4

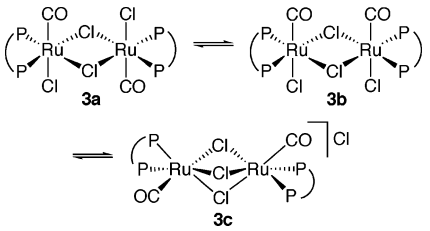

quantitative crystallization of **3c** from benzene solutions containing all three species, (b) observation of all three species by ^{31}P NMR analysis on redissolving **3c** in THF or chlorobenzene, (c) complete transformation of **3a/3b** into **3c** on stripping off the solvent and redissolving in $CDCl_3$, and (d) quantitative transformation of **3a**−**c** into **3c**·PF_6 by reaction with $TlPF_6$, as noted above. Neither the ^1H NMR nor the IR spectra differ appreciably among isomers **3a**−**c**. ^{13}C NMR data for **3a** and **3b** in C_6D_6 could not be obtained, owing to crystallization of **3c** over several hours in solution, which rapidly depletes the solute concentration.

Attempts to quantify the energy barriers relating **3a**−**c** by variable-temperature ^{31}P NMR experiments in chlorobenzene were hampered by the low solubility of **3c**, which unexpectedly precipitated at elevated temperatures. The complexity of the NMR spectrum, resulting from dynamic exchange between four sites with mutual coupling between two (P_A and P_B of **3c**), exceeds current capabilities for line shape analysis. Some insight can be gleaned from reactivity studies, however. Complex **3c** is considerably less reactive than its edge-sharing isomers, as indeed the EXSY data suggest. It is air-stable *in solution* in $CDCl_3$ over a period of weeks and remarkably resistant to reaction with carbon monoxide: carbonylation of **3c** (as a homogeneous solution in $CDCl_3$) required 4 days for complete conversion to **4** at 22 °C. The robustness of the $Ru_2(\mu\text{-}Cl_3)$ entity is implied by a number of other reports. Dimer **6**, for example (PP = (*R*,*R*)-3-benzyl-2,4-bis(diphenylphosphino)pentane; Scheme 5), requires several hours to convert into edge-sharing **7a** even at 90 °C in neat DMSO,[39] while the vinylidene complex $\{[Ru(dcypb)(=C=CH^tBu)]_2(\mu\text{-}Cl_3)\}Cl$ is only ca. 30% converted to mononuclear species after 48 h under CO in refluxing chlorobenzene.[44] As noted in the Introduction, the triply bridged alkylidene complexes $RuCl(PP)(\mu\text{-}Cl_3)Ru(PP)(=CHR)$ represent a catalyst sink in olefin metathesis: these species react very sluggishly even toward the strained, notoriously reactive monomer norbornene,[23] in sharp contrast to the high ROMP activity reported by Hofmann et al. for the doubly bridged $\{[Ru(PP)(CHR)]_2(\mu\text{-}Cl_2)\}^{2+}$ complexes.[24] Illustrative of the thermodynamic stability of the $Ru_2(\mu\text{-}Cl)_3$ moiety is the very high efficiency of routes to such species from a range of precursors, including edge-bridged dimers.[45−47] Severin has contrasted the irreversibility of this reaction with the lability of the corresponding $MM'(\mu\text{-}Cl)_2$ products,[46] while Caulton and co-workers have likewise noted that $M_2(\mu\text{-}Cl_2)$ units readily undergo bridge-cleaving reactions.[48]

Scheme 5

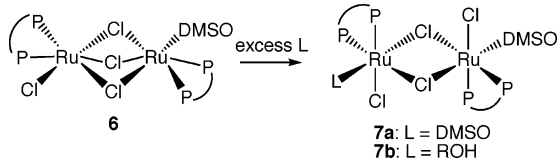

Consistent with the higher reactivity of the edge-bridged dimers **3a** and **3b** is the accelerated rate of carbonylation of **3** in THF, in which all three isomers

(41) Recent attempts to isolate the dimeric species instead led to crystallographic characterization of $[Ru_2(\mu\text{-}Cl)_3(CO)_2(PP)_2][RuCl_3(CO)(PP)]$,[35] again pointing toward the thermodynamic stability of the face-bridged structural motif.

(42) Bustelo, E.; Jiménez-Tenorio, M.; Puerta, M. C.; Valerga, P. *J. Chem. Soc., Dalton Trans.* **1999**, 2399−2404.

(43) The EXSY experiment also reveals site exchange between the inequivalent phosphines of **3c**, probably owing to motion of the flexible dcypb backbone.

(44) Drouin, S. D.; Foucault, H. M.; Yap, G. P. A.; Fogg, D. E. *Organometallics* **2004**, *23*, 2583−2590.

(45) Quebatte, L.; Scopelliti, R.; Severin, K. *Angew. Chem. Int. Ed.* **2004**, *43*, 1520−1524.

(46) Severin, K. *Chem. Eur. J.* **2002**, *8*, 1514−1518. The catalytic data of ref 45 suggest, however, that heterometallic $MM'(\mu\text{-}Cl)_3$ dimers may be more labile.

(47) Gauthier, S.; Quebatte, L.; Scopelliti, R.; Severin, K. *Chem. Eur. J.* **2004**, *10*, 2811−2821.

(48) Coalter, J. N.; Huffman, J. C.; Streib, W. E.; Caulton, K. G. *Inorg. Chem.* **2000**, *39*, 3757−3764.

are present, vs $CDCl_3$ or CH_2Cl_2 solutions, which contain only **3c**. Use of alcohol solvents similarly promotes reaction: in both cases, formation of **4** is complete within hours, as compared to the time scale of days in $CDCl_3$ noted above. Despite this evidence of their capacity to destabilize the $Ru_2(\mu\text{-}Cl_3)$ moiety, MeOH and THF appear too labile as ligands toward **3** to permit direct observation of the solvento species by NMR analysis. Thus, in THF, only signals for **3a**−**c** are evident; in 1:1 CD_2Cl_2−MeOH, only **3c** is observed (although signals at ca. 23 ppm appear on heating the latter; vide supra). Face-sharing dimers, including the Noyori catalyst described above, have long been known to exhibit amplified hydrogenation activity in the presence of alcohols.[22,39,40] Bianchini's group has correlated this effect with transformation into edge-sharing dimers (e.g. **7b**, Scheme 5) in methanolic solutions: notably, the triply bridged structure was regenerated on removal of solvent.[39] While equilibria between trichloro- and dichloro-bridged species have also been noted in pyridine[49] (and use of acetonitrile solvent transforms the dimers into mononuclear species),[39,50] the coordinating power of such donors tends to inhibit catalysis. The activating effect of alcohol (co)solvents may thus be due, at least in part, to their capacity to disrupt the triply bridged unit via formation of *labile* Ru−O(H)R bonds. Similar behavior involving water as a transient donor may possibly account for the recent observation that catalysis via $MM'(\mu\text{-}Cl)_3$ dimers is faster in "wet" organic solvents.[47] Conversely, the reactivity (and, by extension, the catalytic activity) of such dimeric species can be expected to be at a minimum in media such as neat $CHCl_3$ and CH_2Cl_2, in which the unreactive, triply bridged isomer is strongly preferred.

Molecular Structures of 3a/3b, 3c, and 4a/4b. ORTEP representations, with relevant bond lengths and angles, are shown for **3a/3b** and **3c** in Figures 1 and 2 and for **4a/4b** in Figure 3. Bond distances and angles for **3c** are given in Table 2. The coordination about each Ru center is distorted octahedral. Complexes **3a/3b** and **3c** are edge-sharing and face-sharing bioctahedra, containing two metal centers bridged by two and three chloride ligands, respectively. Structures **3a/3b** and **4a/4b** are located around a crystallographic center of symmetry, and the terminal Cl(1) and CO ligands are mutually disordered. Consequently, the X-ray data do not distinguish between transoid and cisoid isomers **3a** and **3b** (as also noted for the edge-sharing dimer $[RuCl(P^tBu_2Me)_2(CO)]_2(\mu\text{-}Cl)_2$[27]) or between *ccc*-**4a** and *tcc*-**4b**, and bond distances and angles involving the disordered atoms are not meaningful.

A search of the Cambridge Crystallographic Database suggests that the unsupported, edge-bridged structural motif represented by $[RuCl_2LL'L'']_2(\mu\text{-}Cl)_2$ (where any of L, L′, and L″ may be identical) is rather rare: only a handful of examples are found,[27,30,33,51−54] most of which

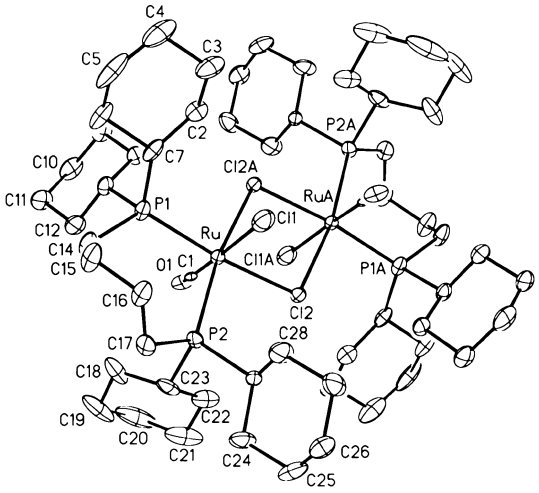

Figure 1. ORTEP diagram for $[RuCl(dcypb)(CO)]_2(\mu\text{-}Cl)_2$ (**3a/3b**). Thermal ellipsoids are shown at the 30% probability level; hydrogen atoms are omitted for clarity. The predominantly chloride site shown for Cl(1) has a true occupancy of 70% Cl. Selected bond lengths (Å) and angles (deg): Ru−P(1), 2.3336(15); Ru−P(2), 2.3645(14); Ru−Cl(2), 2.4643(13); P(1)−Ru−Cl(2), 173.27(5); Cl(2)−Ru−Cl(2A), 80.91(4); P(2)−Ru−Cl(2A), 168.83(5); Ru−Cl(2)−Ru(A), 99.09(4); P(1)−Ru−P(2), 98.61(5).

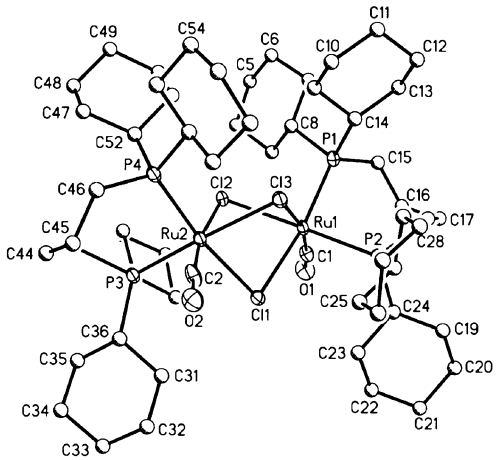

Figure 2. ORTEP diagram for $\{[Ru(dcypb)(CO)]_2(\mu\text{-}Cl)_3\}$-Cl (**3c**). Thermal ellipsoids are shown at the 30% probability level; hydrogen atoms, chloride counterion, and cocrystallized solvent molecules are omitted for clarity. Selected bond lengths and angles are summarized in Table 2.

are isostructural with **3a** or **3b**, though $[RuCl(NN)(CO)]_2(\mu\text{-}Cl)_2$ (NN = phen, di-2-pyridyl ketone)[30] reveals a structure corresponding to **3d**. The face-sharing structural motif is considerably more common. Finally, **4a** is one of a small class of Ru(II) bis-CO compounds containing cis phosphines;[33,34,55,56] two other complexes of this type have been characterized crystallographically.[33,57]

The increased splay of the bridging chlorides in **3a/3b** vs **3c** (Ru−Cl(2)−Ru(A) = 99.09(4)° vs a range of

(49) MacFarlane, K. S.; Thorburn, I. S.; Cyr, P. W.; Chau, D. E. K. Y.; Rettig, S. J.; James, B. R. *Inorg. Chim. Acta* **1998**, *270*, 130−144.
(50) Fogg, D. E.; James, B. R. *Inorg. Chem.* **1997**, *36*, 1961−1966.
(51) Chung, M.-K.; Ferguson, G.; Robertson, V.; Schlaf, M. *Can. J. Chem.* **2001**, *79*, 949−957.
(52) Teulon, P.; Roziere, J. *J. Organomet. Chem.* **1981**, *214*, 391−397.
(53) Southern, T. G.; Dixneuf, P. H.; Le Marouille, J.-Y.; Grandjean, D. *Inorg. Chem.* **1979**, *18*, 2987−2991.
(54) Cotton, F. A.; Matusz, M.; Torralba, R. C. *Inorg. Chem.* **1989**, *28*, 1516−1520.
(55) Whittlesey, M. K.; Perutz, R. N.; Virrels, I. G.; George, M. W. *Organometallics* **1997**, *16*, 268−274.
(56) Mague, J. T.; Mitchener, J. P. *Inorg. Chem.* **1972**, *11*, 2714−2720.
(57) De Araujo, M. P.; Porcu, O. M.; Batista, A. A.; Oliva, G.; Souza, D. H. F.; Bonfadini, M.; Nascimento, O. R. *J. Coord. Chem.* **2001**, *54*, 81−94.

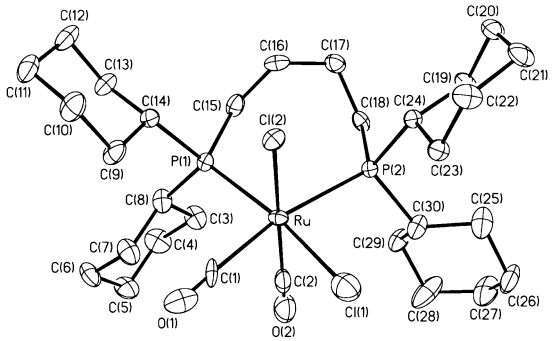

Figure 3. ORTEP diagram for $RuCl_2(dcypb)(CO)_2$ (**4a/4b**). Thermal ellipsoids are shown at the 30% probability level; solvate molecules and hydrogen atoms are omitted for clarity. The predominantly chloride site shown as Cl(1) has a true occupancy of 66% Cl. Selected bond lengths (Å) and angles (deg): Ru−P(1), 2.4101(10); Ru−P(2), 2.4816(10); Ru−Cl(2), 2.4350(10); P(1)−Ru−P(2), 100.50(3).

Table 2. Selected Bond Lengths (Å) and Angles (deg) for Complex 3c

	Bond Distances		
Ru(1)−P(1)	2.335(4)	C(2)−O(2)	1.163(14)
Ru(1)−P(2)	2.352(4)	Ru(1)−Cl(1)	2.478(3)
Ru(2)−P(3)	2.346(4)	Ru(1)−Cl(2)	2.501(3)
Ru(2)−P(4)	2.327(3)	Ru(1)−Cl(3)	2.481(3)
Ru(1)−C(1)	1.856(15)	Ru(2)−Cl(1)	2.485(3)
Ru(2)−C(2)	1.812(14)	Ru(2)−Cl(2)	2.463(3)
C(1)−O(1)	1.124(14)	Ru(2)−Cl(3)	2.495(3)
	Bond Angles		
C(1)−Ru(1)−P(1)	91.2(4)	P(2)−Ru(1)−Cl(1)	96.09(12)
C(1)−Ru(1)−P(2)	91.9(4)	P(1)−Ru(1)−Cl(3)	98.45(12)
C(2)−Ru(2)−P(4)	90.4(4)	P(2)−Ru(1)−Cl(3)	95.53(12)
P(1)−Ru(1)−Cl(1)	171.52(12)	P(1)−Ru(1)−P(2)	92.21(12)
P(2)−Ru(1)−Cl(2)	172.02(13)	C(2)−Ru(2)−P(3)	92.1(4)
P(4)−Ru(2)−Cl(1)	171.32(12)	O(1)−C(1)−Ru(1)	173.2(13(1)
P(3)−Ru(2)−Cl(3)	170.25(12)	O(2)−C(2)−Ru(2)	175.4(12)

85.57(10)−85.83(10)°, respectively) reflects the greater compactness of the face-sharing structure. This effect is manifested in a significant decrease in the Ru−Ru distance in **3c**, relative to that in **3a/3b** (3.384(4) Å vs 3.7730(13) Å). Structure **3c** exhibits the compression of cofacial Cl−Ru−Cl angles (76.93(11)−80.62(11)°) usual for $Ru_2(\mu\text{-}Cl)_3$ face-sharing bioctahedra;[58] similarly, P−Ru−P angles (average 92.7°) compare well with those in face-bridged $Ru_2Cl_5(dcypb)_2$ (average 94.4°)[25] but are significantly smaller than those for **3a/3b** and **4a/4b** (98.61(5) and 100.50(3)°, respectively). Ru−Cl and Ru−P bond lengths fall within the usual ranges.[58] While C−O, Ru−C, and Ru−Cl(1) bond distances for **3a/3b** and **4a/4b** are obscured by Cl/CO disorder, C−O bond lengths in **3c** (average 1.144 Å) are comparable to those in *mer*,*cis*-$RuCl_2(PPh_2Me)_3(CO)$[31] (1.167 Å) and *ctc*-$[RuCl_2(PhCH_2PPh_2)_2(CO)_2]$ (1.13 Å).[58c]

Conclusions

The foregoing describes convenient routes into monocarbonyl ruthenium complexes containing the basic, bulky diphosphine dcypb. Dimeric $[RuCl_2(PP)(CO)]_2$ can be observed as three geometrically distinct isomers in solution, enabling examination of the relationship between bridging geometry and reactivity. Face-sharing $\{[Ru(dcypb)(CO)]_2(\mu\text{-}Cl)_3\}Cl$ (**3c**) is quite unreactive, relative to its edge-bridged isomers, as evidenced by its stability toward air and its slow rate of carbonylation. These observations are of broader interest in context of catalysis mediated by $Ru_2(\mu\text{-}Cl)_3$ species. Dimerization can, of course, provide a resting state in catalysis (i.e. a "protected" reservoir of the catalytically active monomer). Alternatively, however, it may represent a deactivation pathway, or catalyst sink. The catalytic utility of a coordinatively saturated dimer will in general be limited by its kinetic capacity to provide a binding site via liberation of the coordinatively unsaturated monomer. The higher reactivity of edge-bridged dimers thus reflects the greater lability of the bridging chloride donors. Conversely, the stability of the $Ru_2(\mu\text{-}Cl)_3$ unit may point toward a general obstacle in catalysis mediated by such dimers. The capacity of labile donors such as alcohols or ethers to disrupt the triply bridged unit suggests a straightforward means of amplifying reactivity, as well as a partial explanation for the solvent dependence of catalysis mediated by such species.

Experimental Section

Unless otherwise stated, all operations were performed under N_2 using standard Schlenk or drybox techniques. Dry, oxygen-free solvents were obtained using an Anhydrous Engineering solvent purification system and stored over Linde 4 Å molecular sieves. $CDCl_3$ and C_6D_6 were dried over activated sieves (Linde 4 Å) and degassed by consecutive freeze/pump/thaw cycles. $Ru_2Cl_4(dcypb)_2(N_2)$ (**1**)[25] was prepared according to literature procedures. $RuCl_3 \cdot 3H_2O$ was purchased from Strem Chemicals. CO was obtained from Praxair and used as received. NMR spectra were recorded on a Varian XL-300 spectrometer or Bruker AMX-500 spectrometer. Peaks are reported in ppm, relative to 85% H_3PO_4 (^{31}P) or the deuterated solvent (^1H, ^{13}C). Infrared spectra were recorded on a Bomem MB100 IR spectrometer. Microanalytical data were obtained using a Perkin-Elmer Series II CHNS/O instrument.

Attempted Stoichiometric Carbonylation of RuCl(dcypb)(μ-Cl)$_3$Ru(dcypb)(N_2) (1). Attempts to prepare **3** via reaction of **1** with stoichiometric amounts of CO were unsuccessful. In a representative procedure, **1** (23.0 mg, 18.1 μmol) was suspended in 5.00 mL of C_6D_6, in a flask with total internal volume 25.96 mL. The flask was connected to a high-vacuum line equipped with a digital Baratron capacitance manometer. The suspension was frozen with liquid nitrogen and the flask evacuated to an ultimate vacuum of 38 Torr. Carbon monoxide gas (32 Torr) was then transferred from a glass bulb, following which the system was sealed and warmed to 22 °C. The resulting suspension was stirred for 24 h, over which time the suspension partially cleared, though some orange-brown solid remained undissolved. $^{31}P\{^1H\}$ NMR analysis of an aliquot at this time revealed the presence of **1** (~5% integrated intensity), **2** (5%), **4a** (30%), **4b** (30%), and unidentified product(s) characterized by singlets at 22.7 and 22.8 ppm (30%). These integration ratios are not quantitatively significant, owing to the presence of undissolved **1** and/or **2**.

RuCl(dcypb)(μ-Cl)$_3$Ru(dcypb)(CO) (2). Formaldehyde gas, generated by heating paraformaldehyde at 180 °C under a stream of N_2, was bubbled through a suspension of **1** (50 mg, 0.79 μmol) in 10 mL of benzene. After 30 min, the supply of formaldehyde was stopped, the system sealed, and the suspension stirred for 24 h. Concentration and addition of hexanes afforded an orange-brown solid which was filtered off, washed with hexanes (3 × 5 mL), and dried under vacuum. The poor solubility of the product in all organic solvents

(58) (a) Cotton, F. A.; Torralba, R. C. *Inorg. Chem.* **1991**, *30*, 2196−2207. (b) Rhodes, L. F.; Sorato, C.; Venanzi, L. M.; Bachechi, F. *Inorg. Chem.* **1988**, *27*, 604−610. (c) Wilkes, L. M.; Nelson, J. H.; Mitchener, J. P.; Babich, M. W.; Riley, W. C.; Helland, B. J.; Jacobson, R. A.; Cheng, M. Y.; Seff, K.; McCusker, L. *Inorg. Chem.* **1982**, *21*, 1376−1382.

Table 3. Summary of Crystallographic Data and Structure Refinement Details for [RuCl(dcypb)(CO)]$_2$(μ-Cl)$_2$ (3a/3b), {[Ru(dcypb)(CO)]$_2$(μ-Cl)$_3$}Cl (3c), and RuCl$_2$(dcypb)(CO)$_2$ (4a/4b)

	3a/3b	3c	4a/4b
empirical formula	$C_{58}H_{104}Cl_4O_2P_4Ru_2$	$C_{82}H_{128}Cl_4O_2P_4Ru_2$	$C_{42}H_{64}Cl_2O_2P_2Ru$
formula wt	1301.23	1613.66	834.84
temp, K	203(2)	203(2)	203(2)
wavelength, Å	0.710 73	0.710 73	0.710 73
cryst syst, space group	monoclinic, $C2/c$	monoclinic, $P2_1/n$	orthorhombic, $Pna2_1$
unit cell dimens			
a, Å	26.508(3)	15.3703(19)	15.560(1)
α, deg	90	90	90
b, Å	14.576(2)	18.721(2)	11.522(1)
β, deg	109.078(2)	99.027(3)	90
c, Å	17.037(2)	28.156(4)	23.213(2)
γ, Å	90	90	90
V, Å^3	6221.2(14)	8001.7(17)	4161.9(6)
Z; calcd density, g/cm^3	4; 1.389	4; 1.339	4; 1.332
abs coeff, mm^{-1}	0.799	0.636	0.615
F(000)	2736	3408	1760
cryst size, mm	0.1 × 0.1 × 0.1	0.05 × 0.05 × 0.05	0.2 × 0.2 × 0.2
θ range for data collecn. deg	1.62−28.84	1.31−20.81	1.75−28.82
limiting indices	$-35 \le h \le 33$	$-15 \le h \le 15$	$0 \le h \le 20$
	$0 \le k \le 19$	$0 \le k \le 18$	$0 \le k \le 15$
	$0 \le l \le 22$	$0 \le l \le 28$	$-30 \le l \le 31$
no. of rflns collected/unique	24 591/7487 (R(int) = 0.1291)	63 347/8378 (R(int) = 0.4158)	32 606/9930 (R(int) = 0.0506)
completeness to θ; %	28.84; 91.9	20.81; 100.0	28.82; 94.8
abs cor		semiempirical from equivalents	
max, min transmission	0.928 077, 0.742 233	0.928 076, 0.779 953	0.928 076, 0.731 149
refinement method		full-matrix least squares on F^2	
no. of data/restraints/params	7487/0/316	8378/0/399	9930/1/442
goodness of fit on F^2	1.015	1.002	1.064
final R indices ($I > 2\sigma(I)$)[a]	R1 = 0.0567, wR2 = 0.1016	R1 = 0.0704, wR2 = 0.1533	R1 = 0.0449, wR2 = 0.1040
R indices (all data)	R1 = 0.1325, wR2 = 0.1142	R1 = 0.1639, wR2 = 0.1935	R1 = 0.0583, wR2 = 0.1072
largest diff peak, hole, e/Å^3	0.889, −1.025	0.865, −0.773	0.933, −0.904

[a] Definitions of R indices: $R1 = \sum(F_o - F_c)/\sum(F_o)$; $wR2 = [\sum[w(F_o^2 - F_c^2)^2]/\sum[w(F_o^2)^2]]^{1/2}$.

precluded reprecipitation or measurement of the ^{13}C NMR spectrum. Yield: 40 mg (80%). ^1H NMR ($CDCl_3$): δ 0.7−3.1 (br m, CH_2, Cy of dcypb). $^{31}P\{^1H\}$ NMR (C_6D_6): δ 59.6 (d, $^2J_{PP}$ = 40 Hz, 1P), 50.4 (d, $^2J_{PP}$ = 23 Hz, 1P), 43.7 (d, $^2J_{PP}$ = 40 Hz, 1P), 43.0 (d, $^2J_{PP}$ = 23 Hz, 1P). IR (Nujol, cm^{-1}): ν(CO) 1940 (m). Anal. Calcd for $C_{57}H_{104}OCl_4P_4Ru_2$: C, 53.77; H, 8.23. Found: C, 53.21; H, 8.27.

[RuCl(dcypb)(CO)]$_2$(μ-Cl)$_2$ (3).[20] (a) An orange suspension of **1** (50 mg, 0.039 mmol) in 20 mL of methanol was stirred under 1 atm of CO for 18 h, following which the yellow-white suspension (100% tcc **4b**, as judged by ^{31}P NMR analysis of an aliquot in $CDCl_3$) was heated to reflux under N_2 for 16 h. The solvent was then removed completely, and the residual solid was taken up in benzene to crystallize **3c**. This causes the disappearance of "impurities", possibly $RuCl_2$(dcypb)(CO)(MeOH) (**5**), present in the crude mixture. ^{31}P NMR in 1:1 CH_2Cl_2/MeOH: 23.7 (s), 24.0 ppm (s); 25% of total integration. Inert-atmosphere MALDI MS (CH_2Cl_2; pyrene matrix): *m/z* 1264.9 (cation of **3c**), 621.8 ([**4** − $(CO)_2$]), 614.8 ([**4** − Cl − CO]). Yield of **3c** after washing with benzene (2 mL) and Et_2O (4 × 2 mL) and drying under vacuum: 42 mg (82%). A control experiment carried out by refluxing **1** in MeOH under N_2 showed no carbonylation.

(b) A solution of **4a/4b** (95:5) (42 mg, 0.062 mmol) in 20 mL of MeOH was refluxed under N_2 for 16 h. The solvent was removed under high vacuum to yield a yellow product consisting of solely **3c** (^{31}P NMR). Clean **3c** crystallized on taking up the oil in benzene. Isolated yield: 31 mg (78%). The isomeric form of **3** is solvent-dependent. (i) In $CDCl_3$: $^{31}P\{^1H\}$ NMR ($CDCl_3$, δ) 50.8 (d, $^2J_{PP}$ = 23 Hz, **3c**), 42.5 (d, $^2J_{PP}$ = 23 Hz, **3c**); $^{13}C\{^1H\}$ NMR ($CDCl_3$, δ) 200.3 (t, $^2J_{PC}$ = 15 Hz, *C*O, **3c**). ^1H NMR ($CDCl_3$, δ) 1.10−2.53 (br m, CH_2, Cy of dcypb); IR (Nujol, cm^{-1}) ν(CO) 1958. (ii) In C_6D_6: $^{31}P\{^1H\}$ NMR (C_6D_6, δ) 55.3 (d, **3c**, $^2J_{PP}$ = 23 Hz), 42.3 (d, **3c**, $^2J_{PP}$ = 23 Hz), 40.6 (s, **3a** or **3b**), 34.4 (s, **3a** or **3b**). ^1H NMR and IR spectra are indistinguishable from those in (i). The concentration of solute is rapidly depleted by crystallization of **3c** (identified by X-ray diffraction), precluding measurement of the $^{13}C\{^1H\}$ NMR spectrum. (iii) In chlorobenzene: $^{31}P\{^1H\}$ NMR (C_6H_5Cl, δ) 52.2 (d, **3c**, $^2J_{PP}$ = 25 Hz), 42.5 (d, **3c**, $^2J_{PP}$ = 25 Hz), 39.0 (s, **3a** or **3b**), 32.7 (s, **3a** or **3b**).

One-Pot Synthesis of 3c from RuCl$_2$(PPh$_3$)$_3$. Addition of solid dcypb (104 mg, 0.23 mmol) to a solution of $RuCl_2(PPh_3)_3$ (200 mg, 0.21 mmol) in 5 mL of benzene caused an instantaneous color change from dark brown to green. The solution was stirred under N_2 for 8 h, following which MeOH (20 mL) was added to the orange suspension and the atmosphere was exchanged for CO. A clear yellow solution formed on stirring overnight. This was heated to reflux under N_2 for 8 h, stripped of solvent, and taken up in benzene, from which clean **3c** crystallized as above. Yield after filtering and washing with diethyl ether (5 × 5 mL): 99 mg (72%).

{[Ru(dcypb)(CO)]$_2$(μ-Cl)$_3$}PF$_6$ (3c(PF$_6$)). A solution of $TlPF_6$ (20 mg, 0.059 mmol) in 2 mL of THF was added to a suspension of **3** (75 mg, 0.12 mmol of Ru) in 6 mL of THF. The suspension was stirred for 16 h and then filtered through Celite and neutral alumina. The filtrate was concentrated and Et_2O added to precipitate a yellow solid. This was filtered off, washed with Et_2O and hexanes, and dried under vacuum. Recrystallization from THF/Et_2O afforded clean **3c**(PF_6). Yield: 66 mg (81%). $^{31}P\{^1H\}$ NMR (acetone-d_6, δ): 52.7 (d, $^2J_{PP}$ = 24 Hz), 41.6 (d, $^2J_{PP}$ = 24 Hz), −146.3 (sept, $^1J_{PF}$ = 708 Hz). ^1H NMR (acetone-d_6, δ): 1.10−2.59 (br m, CH_2, Cy of dcypb). Spectra in $CDCl_3$ are identical with those for **3c**, neglecting the PF_6 septet. IR (Nujol, cm^{-1}): ν(CO) 1956 (s). Anal. Calcd for $C_{58}H_{104}O_2Cl_3P_5F_6Ru_2$: C, 49.38; H, 7.43. Found: C, 49.63; H, 7.53.

RuCl$_2$(dcypb)(CO)$_2$ (ccc, 4a; tcc, 4b). We earlier described formation of a 1:4 mixture of **4a/4b** by reaction of **1** with CO in THF over 24 h.[25] The same reaction in EtOH permits isolation of **4b**. Treatment of an orange suspension of **1** (50 mg, 0.039 mmol) in 20 mL of EtOH with CO caused a color

change to pale yellow over 18 h at room temperature. The reaction mixture was cooled to −35 °C, and the precipitate was filtered off and washed with EtOH, Et_2O, and then hexanes. Yield of clean **4b** after drying under vacuum: 20 mg (38%). A second crop (1:9 mixture of **4a/4b**) was obtained by concentration and addition of cold pentane. Yield after washing with cold pentane and drying under vacuum: 29 mg (92% total). Spectroscopic data (see Table 1) agree with values previously reported.[25] A $^{31}P-^{31}P$ EXSY experiment shows no correlation between the two isomers.

Solvent Effects in Carbonylation of 3c. A solution of cationic **3c** (45 mg, 0.069 mmol Ru) in 10 mL of $CHCl_3$ was stirred under 1 atm of CO at room temperature. Complete conversion to $RuCl_2(dcypb)(CO)_2$ required 4 days (^{31}P NMR). Concentration and addition of cold pentane produced a pale yellow powder (95:5 **4a/4b**), which was filtered off, washed with pentane, and dried under vacuum. Yield: 42 mg (89%). An identical experiment carried out in 10 mL of THF or EtOH showed complete conversion to **4** within 14 or 18 h, respectively.

Crystallographic Analysis of [RuCl(dcypb)(CO)]$_2$(μ-Cl)$_2$ (3a/3b), {[Ru(dcypb)(CO)]$_2$(μ-Cl)$_3$}Cl (3c), and RuCl$_2$-(dcypb)(CO)$_2$ (4a/4b). X-ray-quality crystals of **3a/3b** deposited under an N_2 atmosphere over 1 month from a benzene solution of **4a** and **4b** (as judged by $^{31}P\{^1H\}$ NMR analysis, which revealed no signals for **3a**−**c**). Diffraction-quality crystals of **4a/4b** were obtained from the same solution over a shorter period. Complex **3c** spontaneously crystallized at room temperature from a C_6D_6 solution containing **3a**−**c**. Details of crystal data and data refinement are collected in Table 3.

Appropriate crystals were selected, mounted on thin glass fibers using viscous oil, and cooled to the data collection temperature. Data were collected on a Bruker AX SMART 1k CCD diffractometer using 0.3° ω scans at 0, 90, and 180° in ϕ. Unit-cell parameters were determined from 60 data frames collected at different sections of the Ewald sphere. Semiempirical absorption corrections based on equivalent reflections were applied.[59] For **3c**, no data were observed beyond 42° (2θ), and the data set was truncated accordingly. Systematic absences in the diffraction data and unit-cell parameters were consistent with *Cc* and *C*2/*c* for **3a/3b**, $Pna2_1$ and *Pnma* (*Pnam*) for **4a/4b**, and, uniquely, with space group $P2_1/n$ (No. 14) for **3c**. Solution in *C*2/*c* for **3a/3b** and $Pna2_1$ for **4a/4b** yielded chemically reasonable and computationally stable results of refinement. The packing diagram for **4a/4b** did not reveal any overlooked crystallographic symmetry, and the absolute structure parameter refined to nil, indicating that the true hand of the data had been determined. The structures were solved by direct methods, completed with difference Fourier syntheses, and refined with full-matrix least-squares procedures based on F^2. The compound molecule for **3a/3b** is located on a 2-fold axis, and a chloride ligand is found disordered with a carbonyl ligand. A chloride ligand is likewise found to be disordered in three positions with two carbonyl ligands in **4a/4b**. The disordered, artificially shortened carbonyl ligands were constrained with an idealized C−O bond distance of 1.145 Å. The isotropic parameters were kept identical for the same atoms in the different disordered positions, and the site occupancies of each contributing disordered position were refined to 72/28 for **3a/3b** and 66/18/16 for **4a/4b**. Two symmetry-unique benzene solvent molecules were found cocrystallized in **4a/4b**. For **3c**, a chloride counterion and four cocrystallized benzene solvent molecules were located in the asymmetric unit. To conserve a favorable data to parameter ratio, all of the non-carbonyl carbon atoms in **3c** were refined isotropically and all phenyl groups were refined as idealized, rigid, flat hexagons; all non-hydrogen, non-carbon atoms and the carbonyl carbon atoms were refined with anisotropic displacement coefficients. All hydrogen atoms were treated as idealized contributions. All scattering factors are contained in the SHELXTL 6.12 program library.[60]

Acknowledgment. This work was supported by the Natural Sciences and Engineering Research Council of Canada, the Canada Foundation for Innovation, and the Ontario Innovation Trust.

Supporting Information Available: ORTEP diagrams and tables of crystal data collection and refinement parameters, atomic coordinates, bond lengths and angles, anisotropic displacement parameters, and hydrogen coordinates for **3a/3b**, **3c**·$4C_6H_6$, and **4a/4b**·$2C_6H_6$; crystal data are also available as CIF files. This material is available free of charge via the Internet at http://pubs.acs.org. The supplementary crystallographic data for this paper also appear in CCDC publications # 264682 (**3a/3b**), 183209 (**3c**), and 264681 (**4a/4b**). These data can be obtained free of charge from the Cambridge Crystallographic Data Centre via www.ccdc.cam.ac.uk/data_request/cif.

OM050195P

(59) Blessing, R. *Acta Crystallogr.* **1995**, *A51*, 33.

(60) Sheldrick, G. M. SHELXTL 6.12; Bruker AXS, Madison, WI, 2001.